ELSEVIER

Journal of Power Sources 105 (2002) 35–44

JOURNAL OF POWER SOURCES

www.elsevier.com/locate/jpowsour

Current distribution over the electrode surface in a lead-acid cell during discharge

Petr Král[a], Petr Křivák[a,*], Petr Bača[a], Milan Calábek[a], Karel Micka[b]

[a]*Department of Electrotechnology, Technical University, Údolní 53, 602 00 Brno, Czech Republic*
[b]*J. Heyrovský Institute of Physical Chemistry, Dolejškova 3, 182 23 Prague 8, Czech Republic*

Received 10 June 2001; received in revised form 27 August 2001; accepted 18 September 2001

Abstract

The current distribution over the plate surface in lead-acid cells in the course of discharge was determined mathematically by using the equivalent circuit method. The dependence of the internal cell resistance on the current and charge passed was determined by measurements on a laboratory cell. Six cell variants were considered differing by the location of tabs serving as current terminals. The results are presented in the form of 3D diagrams at various states of discharge. To make the current distribution nearly uniform, extended current tabs located at opposite ends of the plate electrodes were proposed.

Keywords: Grid design; Current distribution; Lead-acid cell

1. Introduction

At higher discharge rates, the performance of lead-acid batteries may be adversely affected by non-uniform current distribution over the plate surface owing to Ohmic losses in the solid phase. A simplified theory of this phenomenon, which impairs the utilization of the active material, was presented by Dasoyan and Aguf [1]. Several authors developed for this purpose a rigorous mathematical method [2–4]. We have shown [5] that a cell of a lead-acid battery can be modelled by an electrical equivalent circuit consisting of a pair of commercial lead grids, mutually interconnected by a system of parallel, thin resistance wires. These were designed so as to represent the sum of Ohmic resistances of electrolyte and active mass and of polarisation resistances. The current passing through each of the wires was determined from potential measurements. This approximate method was used to obtain information about the influence of the position of the tabs with current leads. To obtain information about the influence of the charge passed, mathematical methods are more suitable. The results are presented here.

2. Equivalent circuit and input data

The mathematical model was based on an electrical equivalent circuit similar to that used by previous authors [3,4]. A single mesh of this circuit is shown in Fig. 1. It is assumed that the positive and negative grids have equal numbers of meshes of equal forms, thus corresponding, in the geometrical sense, to each other. The nodes are visualised by black points. The ''effective'' Ohmic resistances of the horizontal and vertical half grid members including active mass are denoted as R_x and R_y, respectively, with superscript (+ or −) referring to the plate sign. The internal resistance of an elementary section of the electrode system is denoted as R_V with a whole-numbered subscript (k, $k+1$, etc.). Similarly, the electrode potentials at the nodes are denoted as V or W with a whole-numbered subscript, and the currents flowing through the internal resistances R_{V_k}, $R_{V_{k+1}}$ are denoted as I_k, I_{k+1}. Thus, the electrode system can be build up by combining a number of three-dimensional meshes shown in Fig. 1. An analogous equivalent circuit was build up from Ohmic resistors in our previous work [5].

The resistances, R_{V_k}, between the nodes, i.e. between the electrode elements (Fig. 1) were now considered as functions of the current, I_k, and charge passed, Q_k, corresponding to kth node. To obtain an analytical expression for this function, the time course of the internal resistance of a

* Corresponding author.
E-mail address: krivak@uete.fee.vutbr.cz (P. Křivák).

0378-7753/02/$ – see front matter
PII: S0378-7753(01)00923-5

Nomenclature

a	length of vertical grid member
b	length of horizontal grid member
C	discharge capacity of model cell
d	thickness of active mass layer
G_h	conductance of horizontal grid member
G_h^*	conductance of horizontal grid member including negative active mass
G_{ha}	conductance of horizontal column of negative active mass
G_v	conductance of vertical grid member
G_{va}	conductance of vertical column of negative active mass
G_v^*	conductance of vertical grid member including negative active mass
I	total cell current
I_k	current flowing through internal resistance R_{V_k}
Q	total charge passed (It)
Q_k	charge passed due to current I_k
R_x	(with grid sign as superscript) Ohmic resistance of horizontal half grid member
R_y	(with grid sign as superscript) Ohmic resistance of vertical half grid member
R_{V_k}	Ohmic resistance of kth elementary electrode system section
t	time of current passage
U_k	voltage between kth positive and negative nodes
V_k	electrode potential at kth positive node
W_k	electrode potential at kth negative node
x	horizontal coordinate axis
y	vertical coordinate axis
σ	conductivity of negative active mass

laboratory cell (including the electrolyte, interphase, active mass, and polarisation resistances) was measured at various discharge currents. The cell was assembled from five positive and six negative electrodes of dimensions 10 mm × 15 mm (with a Daramic separator) cut out from commercial SLI grids (i.e. two meshes each) and connected in parallel. The electrolyte was H_2SO_4 of 1.28 g/cm^3 density. The cell was discharged, in turn, with currents of 0.1, 0.15, 0.2, 0.3, and 0.35 A. The internal cell resistance was determined at 10 min. intervals by lowering the discharge current for a moment to one-half, thus producing a current drop, ΔI, and recording the voltage change, ΔU. The sought resistance value was set equal to $\Delta U/\Delta I$. It was taken into account that the resistance of the experimental cell was by the factor of 0.1 lower (and the current by the factor of 10 higher) than that of the cell element in Fig. 1. Thus, we arrived at the value of R_{V_k} corresponding to this cell element. The results were expressed by the following regression function calculated by the least squares method:

$$R_{V_k} = 0.32 + 4.2Q_k + 2.6 \times 10^{-5} \exp(730Q_k + 100I_k - 14) \quad (1)$$

The smoothed dependence of R_{V_k} on Q_k at various discharge currents is illustrated in Fig. 2. It is apparent that the most significant increase of the resistance takes place when the end of discharge is approached. A very similar behaviour was observed by Winsel and coworkers [6,7], who measured the sum of interphase (contact) and active mass resistances, and by Hollenkamp et al. [8], who studied the interphase resistance between lead grid and active mass. An exponential dependence of the resistance on the degree of discharge was also found by Bouet [9]. It is also apparent that the resistance increase occurs earlier at higher currents (Fig. 2). This may be attributed to the fact that the current distribution in the active mass becomes more non-uniform at higher currents, causing preferential discharge of the "outer" active mass layer. Accordingly, the resistance of this layer increases more considerably, and this effect is reflected by the behaviour of the R_{V_k} values.

With the positive plate, the active mass does not contribute significantly to the conductance of the grid members. However, with the negative, the grid member conductances

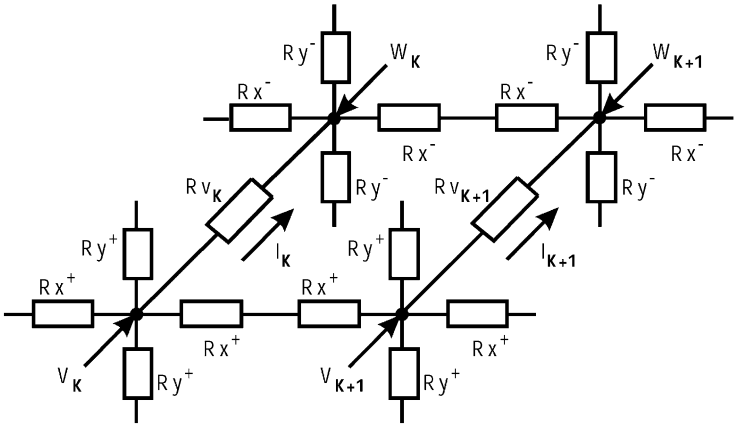

Fig. 1. Part of the equivalent circuit used for calculation of the current distribution over the electrode surface. R_{V_k} resistance between two electrode elements (Eq. (1)). Positive grid: $R_x^+ = 1.6125$ mΩ, $R_y^+ = 0.5375$ mΩ; negative grid (with active mass in the charged state): $R_x^- = 1.327$ mΩ, $R_y^- = 0.327$ mΩ; frame: $R_{x0} = 0.5375$ mΩ, $R_{y0} = 0.3583$ mΩ.

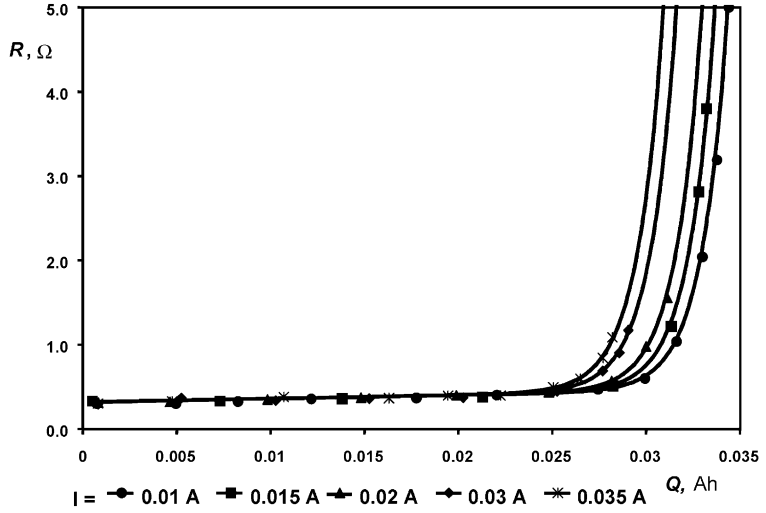

Fig. 2. Dependences of the internal resistance of a cell element on the charge passed for discharge currents rising from 0.01 to 0.035 A. Experimental points are fitted with regression curves based on Eq. (1).

must be corrected for the conductance of the active mass. This can be done approximately as follows: [3].

The negative plate electrode contains vertical grid members of length a and horizontal grid members of length b, and an active mass layer of thickness d and conductivity σ (measured in $\Omega^{-1}\,\mathrm{cm}^{-1}$). We shall consider a column of active mass of thickness d, height a, and width b, surrounding a vertical grid member of length a. The conductance of this column in vertical direction, G_{va} (measured in Ω^{-1}), is given as

$$G_{\mathrm{va}} = \sigma\, d\, \frac{b}{a} \tag{2}$$

Such a column can be assigned to each vertical grid member except for the vertical frame members, to which only one-half of the column of width $b/2$ belongs. If we denote the conductance of the vertical grid member as G_{v}, the conductance of this grid member with the active mass will approximately be given by the equation

$$G^{*}_{\mathrm{v}} = G_{\mathrm{v}} + G_{\mathrm{va}} = G_{\mathrm{v}} + \sigma\, d\, \frac{b}{a} \tag{3}$$

Similarly, we may consider a column of active mass of thickness d, height a and width b, surrounding a horizontal grid member of length b. The conductance of this column in horizontal direction, G_{ha}, is given as

$$G_{\mathrm{ha}} = \sigma\, d\, \frac{a}{b} \tag{4}$$

One-half of such a column of height $a/2$ can be assigned to the horizontal frame members. By analogy to Eq. (3), the conductance of a horizontal grid member with the active mass can approximately be written as

$$G^{*}_{\mathrm{h}} = G_{\mathrm{h}} + G_{\mathrm{ha}} = G_{\mathrm{h}} + \sigma\, d\, \frac{a}{b} \tag{5}$$

The following parameter values were used in the calculations: $a = 0.5$ cm, $b = 1.5$ cm, $d = 0.1$ cm, $\sigma = 2000\,\Omega^{-1}\,\mathrm{cm}^{-1}$. The latter value was taken from the [3] and checked by comparing the calculated potential drop within the negative plate with the measured one. The conductances of the grid members were determined as $G_{\mathrm{v}} = 930\,\mathrm{S}$ and $G_{\mathrm{h}} = 310\,\mathrm{S}$. In accord with our earlier work [10], the conductance of the negative active mass decreases practically linearly with the charge passed, Q, during constant-current discharge; the end value for $Q = 0.035$ Ah equals 0.4 times the starting value. Thus, with the help of the definitions (3) and (5), we obtain $G_{\mathrm{va}} = \sigma d(b/a) = 600 - 10\,286Q$ and $G_{\mathrm{ha}} = \sigma d(a/b) = 66.67 - 1142.9Q$. Now, Eqs. (3) and (5) can be put into the form

$$G^{*}_{\mathrm{v}} = 1530 - 10\,286Q \tag{6}$$

$$G^{*}_{\mathrm{h}} = 376.67 - 1142.9Q \tag{7}$$

Hence, the dependences of the resistances in Fig. 1 on the charge passed at kth node, Q_k, can be expressed by the following approximate equations:

$$R^{-}_{x} = \left(\frac{0.5}{376.67 - 1142.9Q_k}\right) \tag{8}$$

$$R^{-}_{y} = \left(\frac{0.5}{1530 - 10\,286Q_k}\right) \tag{9}$$

where $Q_k = \int I_k\,\mathrm{d}t$ and I_k is generally different for different nodes; in other words, these two quantities depend on the x and y coordinates (used in 3D diagrams, Figs. 3–8).

3. Method of calculation

By applying the first and second Kirchhoff laws to the nodes and loops of the whole equivalent circuit, a system of

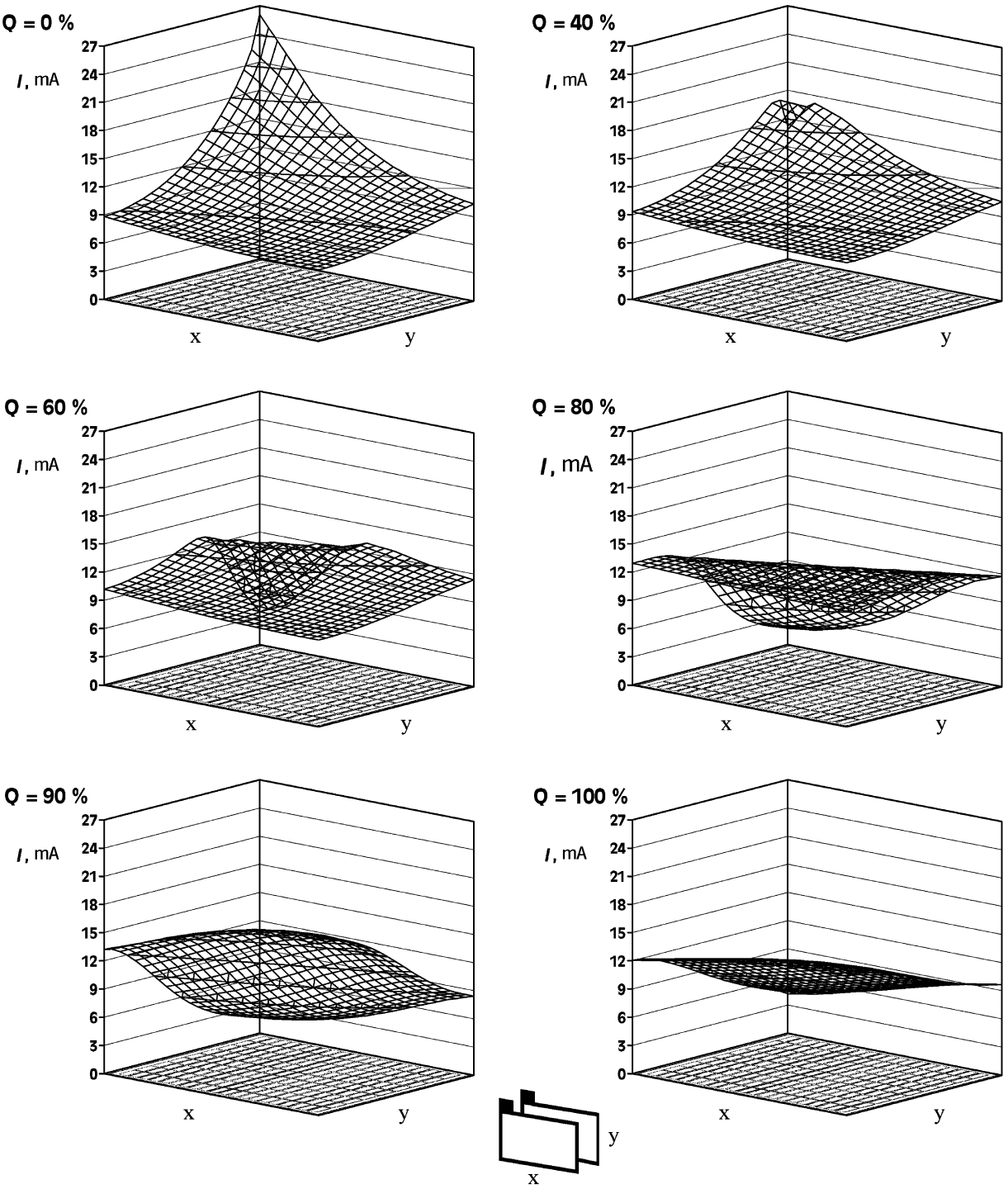

Fig. 3. Current distribution over the plate electrode surface at increasing state of discharge, Q, from 0 to 100% for the most unfavourable tab configuration (units on x and y axes are arbitrary in this and subsequent figures).

linear equations is obtained, whose solution gives the sought distribution of potentials and currents. To take into account the system changes with the time, the calculations were carried out in steps as follows.

- *Step* 1 ($i = 1$, $t_1 = 1$ s, $\Delta t_1 = 1$ s): The initial value of $R_1 = 0.32\,\Omega$ is introduced into all elements representing the internal resistance R_{V_k} and the potential distribution in the nodes of the equivalent circuit is calculated. The node potentials of kth element, V_k^1 and W_k^1, are used to calculate the corresponding voltage and current

$$U_k^1 = V_k^1 - W_k^1, \qquad I_k^1 = \frac{U_k^1}{R_k^1} \tag{10}$$

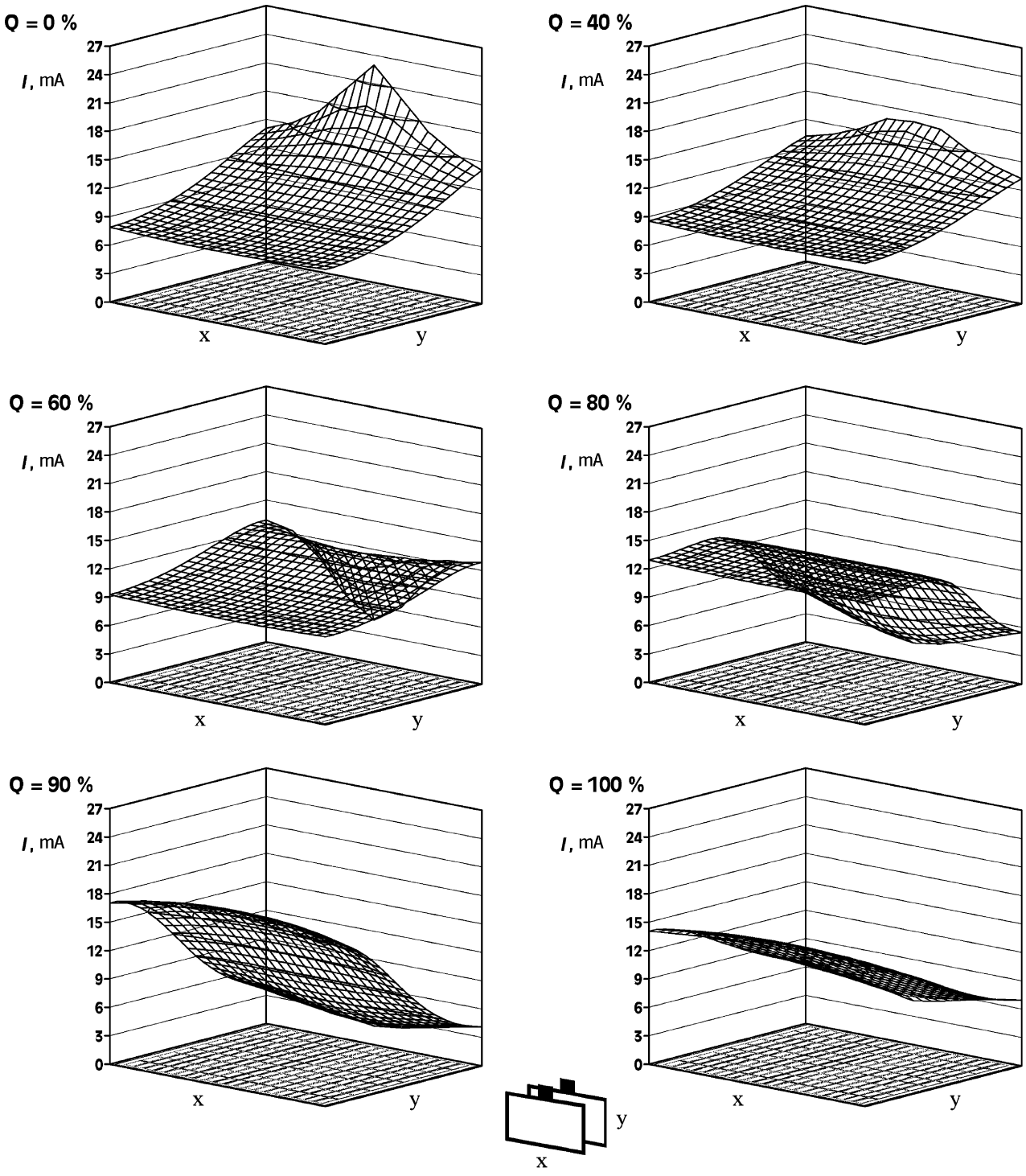

Fig. 4. Current distribution over the plate electrode surface at increasing state of discharge, Q, from 0 to 100% for the tab configuration shown.

The charge passed through the kth element can be calculated from the current as

$$Q_k^1 = I_k^1 \, \Delta t_1 \tag{11}$$

- *Step* 2 ($i = 2$, $t_2 = 30$ s, $\Delta t_2 = t_2 - t_1$): The internal resistance corresponding to the kth element is calculated from Eq. (1). Afterwards, the node potential distribution is again calculated and the corresponding voltage and current values are found as in step 1. The charge passed through the kth element is then calculated as

$$Q_k^2 = Q_k^1 + I_k^2 \, \Delta t_2 \tag{12}$$

The procedure continues step by step until $t_n = 12{,}000$ s.

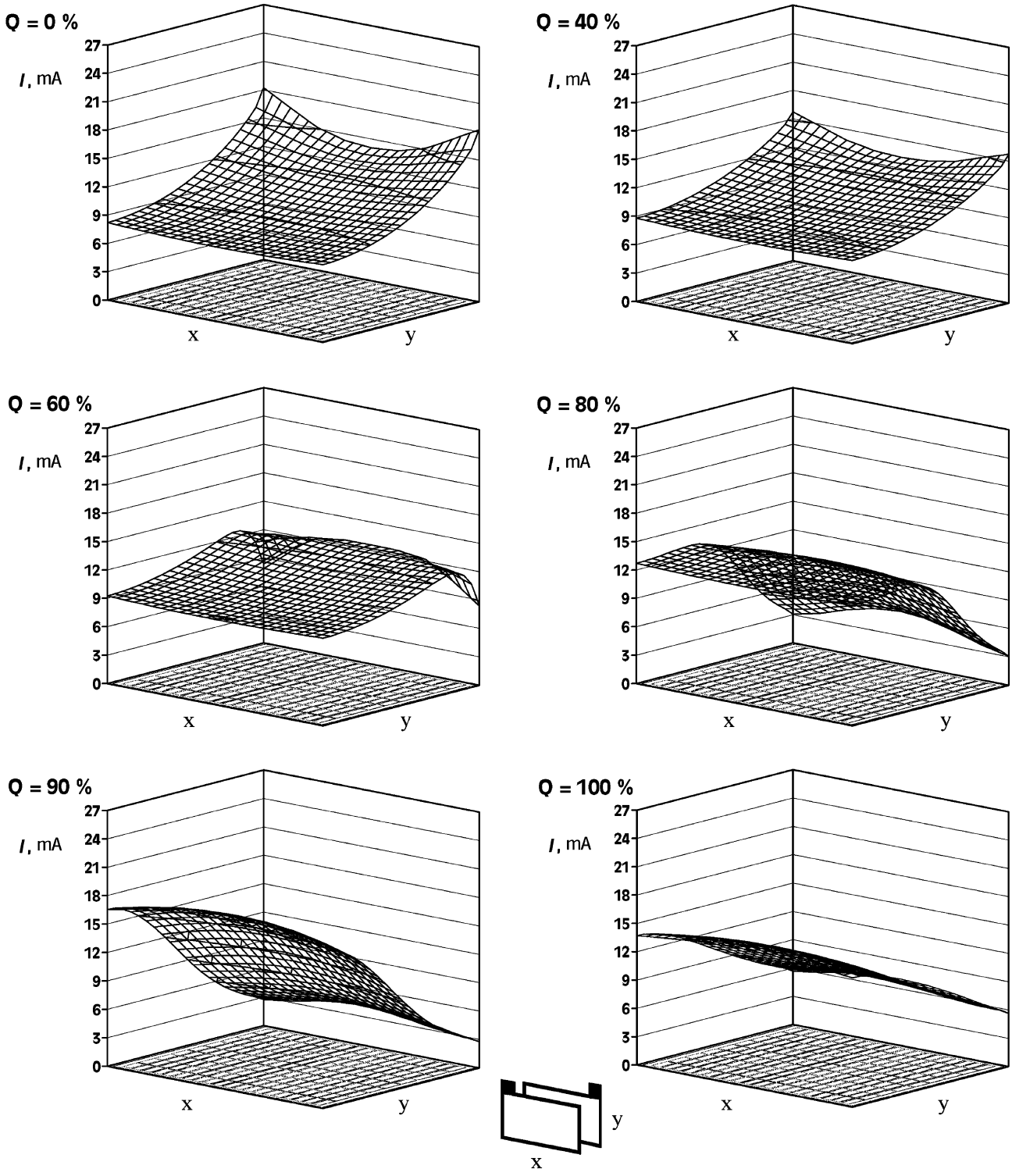

Fig. 5. Current distribution over the plate electrode surface at increasing state of discharge, Q, from 0 to 100% for the tab configuration used in practice.

The chosen value of $\Delta T = 30$ s is suitable since the resulting error in the linearisation is negligible. Higher values of ΔT cause increasing errors in the linearisation, lower values lead to a considerable increase of the calculation time.

4. Results and discussion

The calculated current distributions over the plate electrode surface are presented in the form of 3D diagrams in Figs. 3–8 for Q values corresponding to 0, 40, 60, 80, 90,

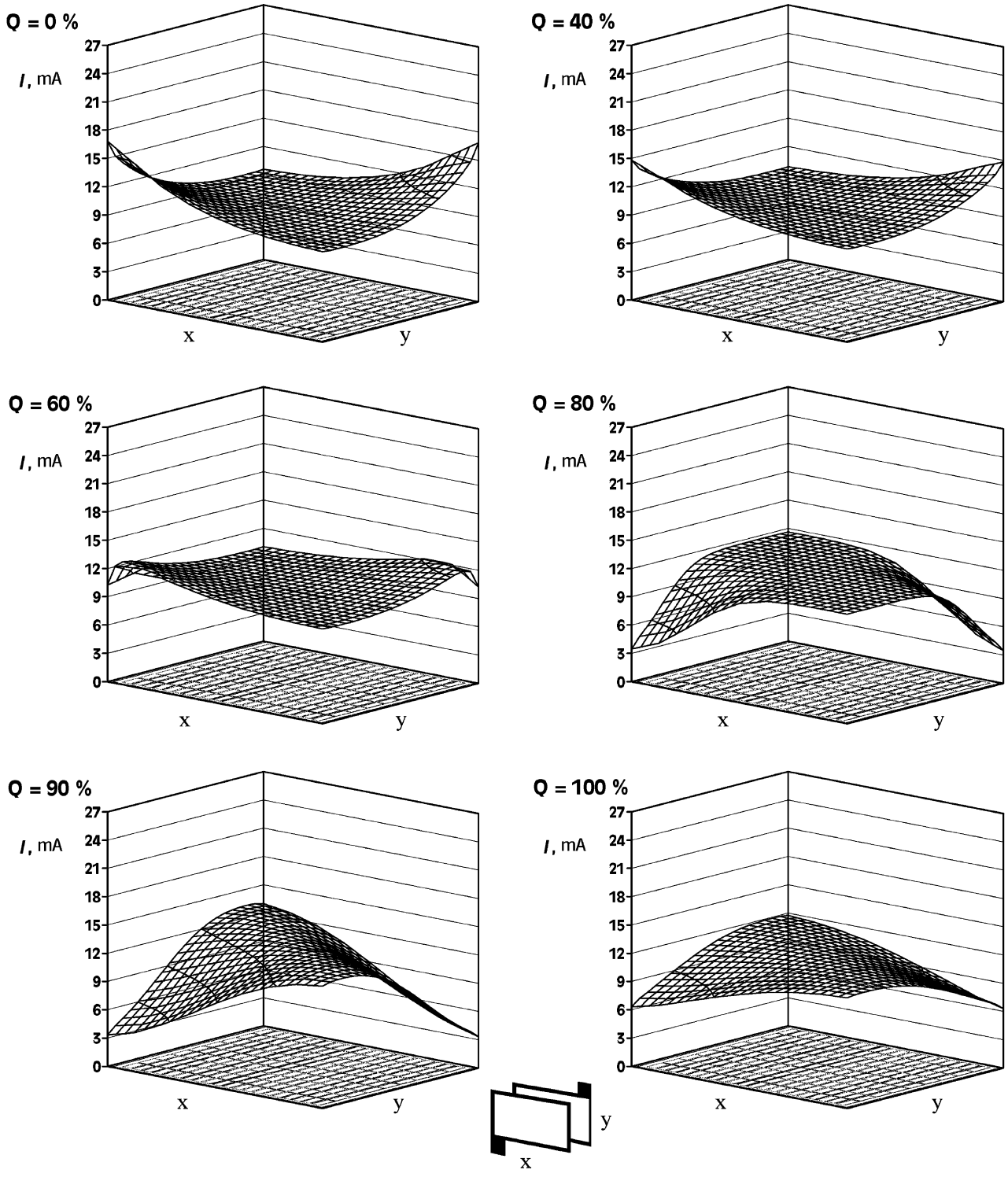

Fig. 6. Current distribution over the plate electrode surface at increasing state of discharge, Q, from 0 to 100% for the tab configuration shown.

and 100% discharge. This corresponds to discharge times of 0, 80, 120, 160, 180, and 200 min, discharge current $I = 2$ A, and discharge capacity $C = 6.66$ Ah. Six configurations of the current tabs welded to the lead grids were considered. These are indicated schematically in the diagrams.

It can be seen that the initial rate of discharge (i.e. the local current) is always more or less elevated in regions close to the tabs. This phenomenon is most pronounced in Fig. 3, where the tabs are located in the corners facing each other. Therefore, this region reaches the discharged state more rapidly. Since the total current is maintained constant, the

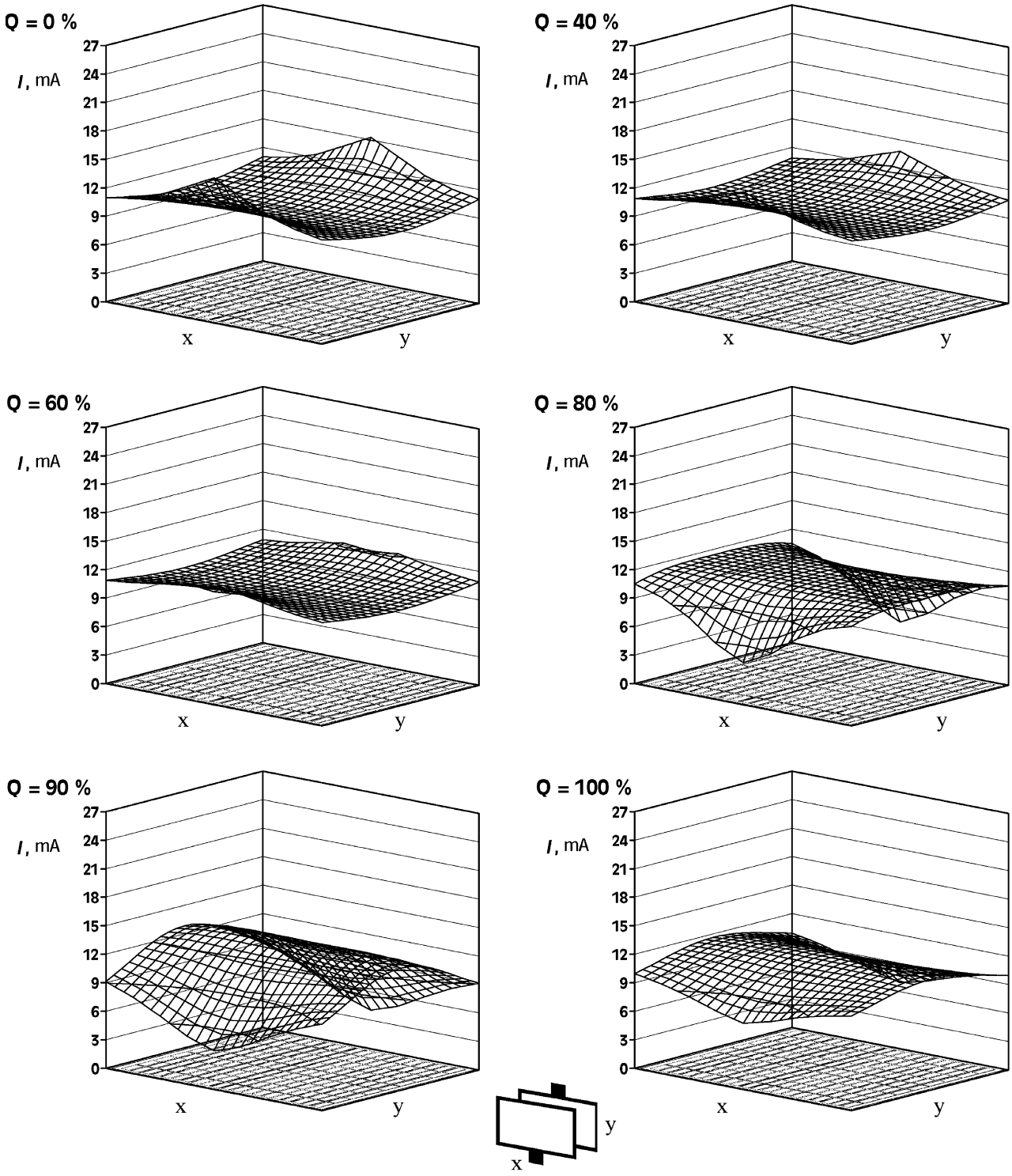

Fig. 7. Current distribution over the plate electrode surface at increasing state of discharge, Q, from 0 to 100% for the tab configuration shown.

current drop in one region causes the discharge rate in another one to increase, although not as much, as can be seen from the diagrams. In spite of this levelling effect, the situation at the end of discharge for most tab configurations (Figs. 3–7) does not look satisfactory. A moderate improvement can be seen from Fig. 7, but the best configuration seems to be the last one, with extended tabs on opposite ends of the plates, corresponding to Fig. 8. This is in accord with the theory presented in our preceding work [5]. Here, the current distribution over the plate surface remains fairly uniform all the time, with a shallow extremum in the middle region of the plates. Since the conductivity of

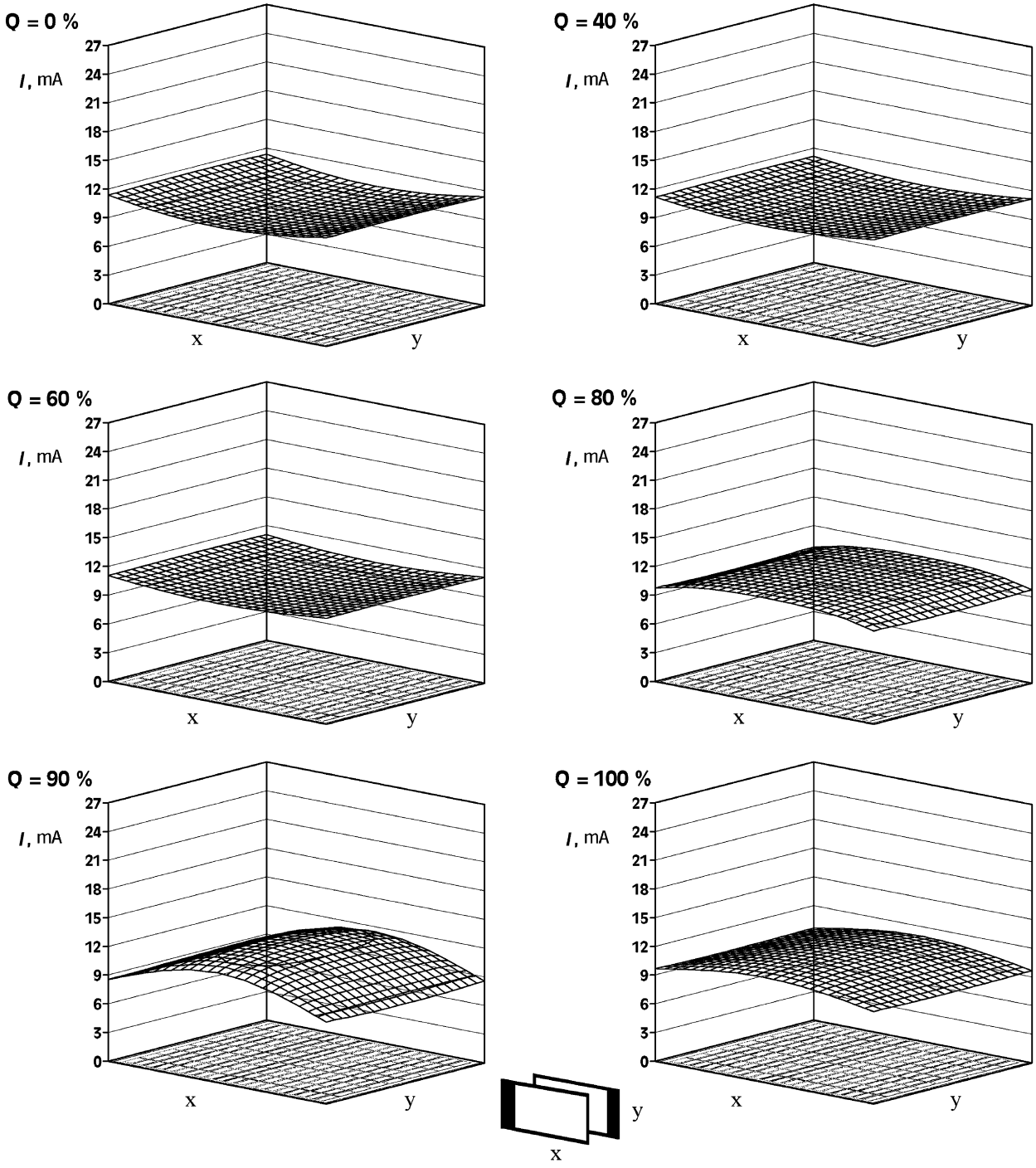

Fig. 8. Current distribution over the plate electrode surface at increasing state of discharge, Q, from 0 to 100% for the most favourable tab configuration.

the negative active mass was taken into account, the negative plate is a better conductor than the positive, resulting in a shift of the position of the extremum toward the tab of the negative electrode (compare the theory in our previous work [5]).

An illustrative criterion characterising the uniformity of the current distribution is the ratio of the maximum to the minimum local currents (I_{max}/I_{min}), which is plotted as a function of the depth of discharge, Q, in Fig. 9 for all the tab configurations under discussion. The configuration used by many manufacturers takes the mean position. The configuration with extended tabs located on opposite ends of the positive and negative plates is obviously by far the best one, since the mentioned criterion is only a little higher than one. Recently, Lam and coworkers [11] proposed a somewhat similar but more complicated arrangement, where the tabs are located at the top and bottom of each of the positive and negative plate electrodes.

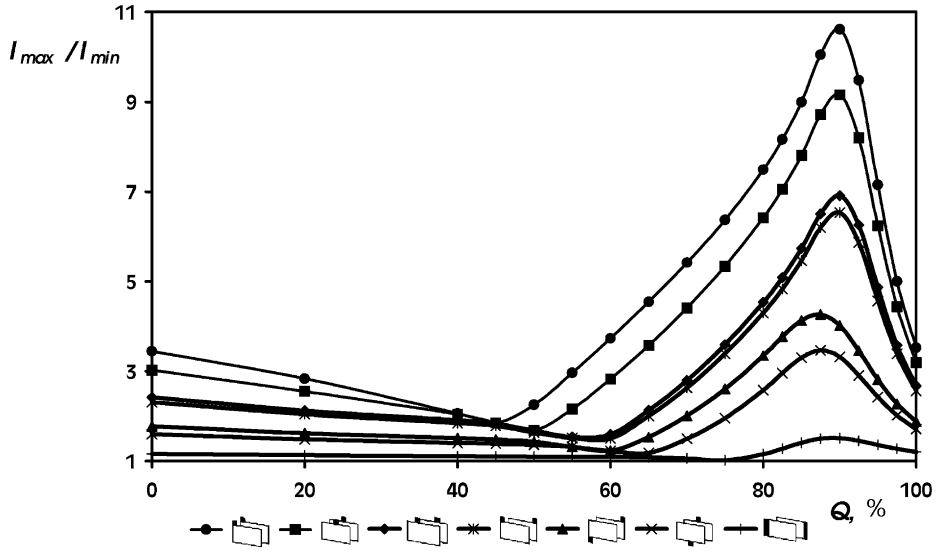

Fig. 9. Dependences of the criterion I_{max}/I_{min} on the relative state of discharge for seven configurations of tabs welded to the lead grids.

Acknowledgements

This work was supported by the Grant Agency of the Czech Republic (Grant no. 102/98/1170).

References

[1] M.A. Dasoyan, I.A. Aguf, Sovremennaya teoriya svincovogo akkumulyatora (Contemporary Theory of Lead-Acid Batteries), Energiya, Leningrad, 1975, p. 84f.
[2] W.H. Tiedemann, J. Newman, F. DeSua, in: D.H. Collins (Ed.), Power Sources, Vol. 6, Academic Press, New York, 1977, p. 15.
[3] W.G. Sunu, B.W. Burrows, J. Electrochem. Soc. 129 (1982) 688.
[4] W.G. Sunu, B.W. Burrows, J. Electrochem. Soc. 131 (1984) 1.
[5] M. Calábek, K. Micka, P. Bača, P. Křivák, J. Power Sources 85 (2000) 145.
[6] A. Winsel, E. Voss, U. Hullmeine, J. Power Sources 30 (1990) 209.
[7] E. Bashtavelova, A. Winsel, J. Power Sources 46 (1993) 219.
[8] A.F. Hollenkamp, K.K. Constanti, M.J. Koop, L. Apateanu, M. Calábek, K. Micka, J. Power Sources 48 (1994) 195.
[9] J. Bouet, J.P. Pompon, Electrochim. Acta 26 (1981) 1477.
[10] M. Calábek, K. Micka, in: K.R. Bullock, D. Pavlov (Eds.), Proceedings of the Symposium on Advanvanced Lead-Acid Batteries, Vol. 84, Part 14, The Electrochemical Society, Pennington, NJ, 1984, p. 288.
[11] L.T. Lam, R.H. Newnham, H. Ozgun, F.A. Fleming, J. Power Sources 88 (2000) 92.